T.B. SETTERSTEN[1],✉
A. DREIZLER[2]
B.D. PATTERSON[1]
P.E. SCHRADER[1]
R.L. FARROW[1]

Photolytic interference affecting two-photon laser-induced fluorescence detection of atomic oxygen in hydrocarbon flames

[1] Combustion Research Facility, Sandia National Laboratories, Livermore, CA 94551, USA
[2] Fachgebiet Energie- und Kraftwerkstechnik, Technische Universität Darmstadt, 64287 Darmstadt, Germany

ABSTRACT This study reports on photochemical interferences affecting atomic oxygen detection using two-photon laser-induced fluorescence at 226 nm. In contrast to previous studies in which molecular oxygen was proven to be the relevant photochemical precursor molecule in a hydrogen-fueled flame, the present investigations were carried out in a laminar diffusion flame of methane and air. The most significant interferences were found at the fuel side of the flame in the absence of molecular oxygen, and vibrationally excited carbon dioxide was identified as the most probable precursor molecule for the photochemical production of oxygen atoms.

PACS 82.50.Hp; 39.30.+w; 32.80.Rm

1 Introduction

Laser-induced fluorescence (LIF) has been proven to be a very useful tool for sensitive detection of atomic oxygen in combustion and plasma environments [1–8]. The excitation wavelengths for single-photon ground-state transitions of atomic oxygen lie in the vacuum ultraviolet (UV), where most practical systems are optically thick. To circumvent this problem, a two-photon excitation scheme is used, taking advantage of the O $3p\ ^3P \leftarrow\leftarrow 2p\ ^3P$ transition at 226 nm, and fluorescence is detected from the $3p\ ^3P \rightarrow 3s\ ^3S$ transition at 845 nm.

The two-photon excitation process requires high pulse irradiance, which can cause photochemical effects in combustion systems. Accurate measurement of atomic oxygen density via two-photon LIF, therefore, requires careful consideration of concomitant processes induced by the laser pulses.

Photolytic interferences have been discussed previously [3, 5, 9–11]. Photolytic production of atomic oxygen has been observed in room-temperature flows [9, 10], and evidence of atomic oxygen production through rapid dissociation after excitation of the O_2 Schumann–Runge bands was observed in lean H_2/O_2 flames [3]. Hydrocarbon flames, however, represent a considerably more complex system, and the source of photolytic production of atomic oxygen has not been characterized in these systems. In the comments of [4] and in [6, 7], some indications are presented showing that additional photochemical interferences occur in hydrocarbon flames, especially for fuel-rich conditions. Investigators have speculated on potentially important precursor molecules, suggesting that CO or CH_2O may contribute to the photolytic signal, but no direct evidence has been presented [6, 7].

Fluorescence interferences have also been observed in flames. These interferences arise mostly from unburned hydrocarbons and exhibit broad absorption and emission features. Fluorescence interferences can be accounted for by either measuring the non-resonant background (detuning the laser from the $3p\ ^3P \leftarrow\leftarrow 2p\ ^3P$ transition) or detecting the fluorescence both on and off the $3p\ ^3P \rightarrow 3s\ ^3S$ transition. Such a correction, however, cannot be used to account for interferences due to photolytic production of atomic oxygen.

The aim of the present study is to identify photolytic precursor molecules in hydrocarbon flames that perturb LIF detection of atomic oxygen. For this purpose a weak picosecond probe laser was used to measure the naturally occurring atomic oxygen profile in a well-documented laminar methane/air diffusion flame [12–14]. Picosecond excitation has a considerable advantage over nanosecond excitation because the photolysis process involves single-photon dissociation of a precursor, while the LIF signal generation involves two-photon absorption; to produce the same LIF signal level, ps excitation requires significantly less pulse energy than is necessary with ns excitation, and therefore ps excitation generates less interference from single-photon photolysis. The variation of the naturally occurring atomic oxygen profile was studied under the action of an intense photolysis laser that was detuned from the atomic oxygen resonance and generated photochemical products. In the following, vibrationally excited CO_2 is identified as the most probable photolytic precursor molecule to oxygen-atom production at 226 nm in a methane/air diffusion flame.

2 Experimental procedure

The experimental arrangement is shown schematically in Fig. 1. It consists of a tunable nanosecond laser,
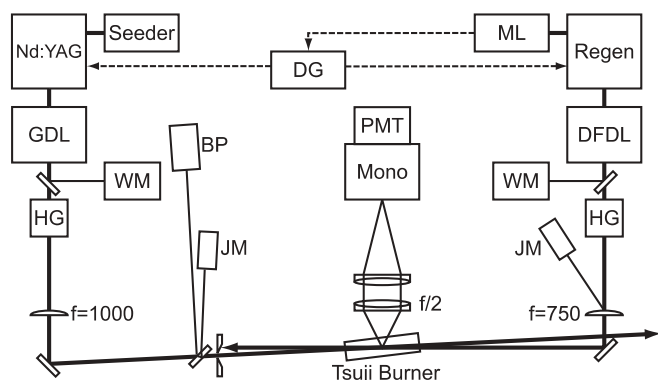
FIGURE 1 A tunable ns laser induces photolysis in the flame and a ps laser probes photolytically produced atomic oxygen via two-photon LIF. GDL: grating dye laser; HG: harmonic generation; ML: mode-locked laser; DFDL: amplified distributed-feedback dye laser; WM: wavemeter; JM: joulemeter; BP: beam profiler; DG: delay generator; Mono: monochromator; PMT: photomultiplier tube

a picosecond laser, a diffusion flame, and a fluorescence detection/recording apparatus. The nanosecond laser pulses induced photolysis in the flame, and the picosecond pulses probed the atomic oxygen concentration.

The photolysis pulses were produced by frequency tripling in BBO crystals the output of a grating-tunable dye laser that was pumped by the 532-nm output of an injection-seeded Nd:YAG laser operating at 20 Hz. The UV pulse width was approximately 3.5 ns, and we estimate that the line width was less than $0.3\,\mathrm{cm}^{-1}$. A half-wave plate/polarizer combination was used to vary the UV pulse energy. A lens with a focal length of 1000 mm focused the UV pulses to a beam diameter of approximately $110\,\mu\mathrm{m}$ at the measurement volume, producing intensities of up to $4\,\mathrm{GW/cm}^2$. The laser wavelength, pulse energy, and beam profile in the measurement volume were continuously monitored during the experiments.

The picosecond probe laser was the same amplified, distributed-feedback dye laser (DFDL) that was used in [15]. Briefly, the DFDL and two amplifier stages were pumped by the second harmonic of a regeneratively amplified Nd:YAG laser operating at 20 Hz. The amplified DFDL output was frequency tripled in two BBO crystals. The resultant pulse width was 55 ps, as measured with a streak camera (Hamamatsu M2547), and we estimated that the UV line width was approximately $1\,\mathrm{cm}^{-1}$, based on the measured line width of the fundamental. The probe laser was tuned to the $J = 2$ line of the $3p\,{}^3P \leftarrow\leftarrow 2p\,{}^3P$ two-photon transition at 225.655 nm. In contrast to observations reported in [5], the line width of the probe laser was sufficiently narrow to avoid excitation of the $O_2(2, 4)P(21)$ line. The probe laser wavelength, line width, and pulse energy were monitored during all experiments. A 750 mm focal length lens focused the beam into the measurement volume. The profile in the measurement volume was approximately Gaussian with a beam diameter of $60\,\mu\mathrm{m}$. Using a half-wave plate and a polarizer, the pulse energy was reduced to $3\,\mu\mathrm{J}$, slightly less than the measured stimulated emission [16] threshold at the peak atomic oxygen concentration in the flame.

The photolysis and probe laser beams were approximately counterpropagating and crossed in the measurement volume with a crossing angle of $0.7°$. The probe laser pulse was delayed by a few ns with respect to the photolysis pulse so as to detect the maximum photochemical interference. Fluorescence from the measurement volume was collected with $f/2$ optics in a direction normal to the probe laser propagation axis. Fluorescence from the $3p\,{}^3P \rightarrow 3s\,{}^3S$ transition of atomic oxygen was passed by a 1/8-m monochromator that produced a 15-nm band pass at 845 nm and was detected with a Hamamatsu R636 photomultiplier tube (PMT). The PMT photocurrent was integrated using a charge-integrating amplifier and then digitized with an oscilloscope. All waveforms were corrected for baseline drifts.

Experiments were carried out in a laminar methane–air diffusion flame that was stabilized on a Tsuji burner [12].

In this geometry, methane flows uniformly from a water-cooled (330 K) porous cylindrical burner that is placed in a laminar flow of air. A laminar diffusion flame forms in the forward stagnation region of the cylinder and, along the symmetry line, the flame can be described very precisely by one-dimensional flame models using detailed molecular transport and chemical reaction schemes [13, 14]. For this work, the methane- and air-flow rates were set to produce a strain rate of $119\,\mathrm{s}^{-1}$, consistent with conditions investigated in [13, 14]. The burner head was rotated horizontally by $20°$ with respect to the laser beams to minimize beam steering due to thermal gradients. The head was traversed vertically by a micrometer to spatially scan the flame through the measurement volume.

3   Results and discussion

The spatial profile of the atomic oxygen concentration along the symmetry line of the flame was recorded by blocking the photolysis laser while allowing the probe laser to excite oxygen atoms in the measurement volume. Sufficiently low probe laser intensities were used so that stimulated emission was completely avoided, the power-law dependence of the LIF signal on the pulse energy was quadratic (1.97 ± 0.05), and lower probe laser intensities produced identical normalized spatial profiles.

The LIF measurements (open circles) are compared with the numerically simulated profile of the oxygen number density (thick solid curve) [14] in Fig. 2. Because few experimental investigations of atomic oxygen quenching have been conducted [4, 8, 9, 17–19], temperature- and species-specific quenching cross sections are very limited. Smyth and Tjossem [7] modeled the quenching conditions in a methane/air diffusion flame and estimated less than 30% variation of the total quenching rate in the vicinity of the atomic oxygen profile. Here, the measurements were normalized to the numerical results, and no attempt was made to account for spatial variation of the fluorescence quenching rate. No measurable fluorescence signal was observed when the probe laser was detuned from the atomic oxygen resonance.
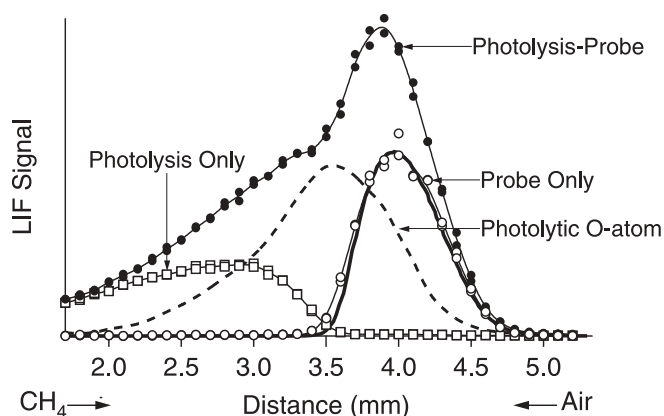
FIGURE 2 LIF signals due to the photolysis laser (*open squares*), the probe laser (*open circles*), and the photolysis and probe lasers (*closed circles*). The *thin solid curves* are smoothing spline fits to the data. The *dashed curve* corresponds to photolytically produced atomic oxygen, obtained by subtracting the photolysis-only and probe-only curves from the photolysis–probe curve. The *thick solid curve* is a numerically simulated profile of the atomic oxygen number density

The non-resonant fluorescence signal due to the photolysis laser is shown as open squares in Fig. 2. In this case the photolysis laser was tuned to 225.579 nm, off-resonant with both O_2 and the atomic oxygen transitions. A laser intensity of 3 GW/cm^2 was employed. On the fuel side of the flame, up to 3.5 mm from the burner surface, fluorescence interferences were observed independently of the photolysis laser wavelength between 225.6 and 226.05 nm. Dispersed fluorescence spectra indicated that this signal was due to broad-band LIF, presumably from unburned and partially oxidized hydrocarbons, that was passed by the 15-nm band pass of the detector. In the vicinity of the naturally occurring oxygen atoms, these interferences were not observed.

When both the photolysis and probe lasers simultaneously interacted in the measurement volume, a dramatic change of the LIF profile was observed (see the filled circles in Fig. 2). The profiles obtained by using either the probe or the photolysis laser individually were smoothed and subtracted from the smoothed photolysis–probe profile to produce the profile shown as the dashed curve in Fig. 2. This remaining contribution is due to photochemically produced oxygen atoms. Note that this profile is peaked on the rich side of the flame.

In previous investigations in the exhaust of a lean H_2/O_2 flame, the photolysis of O_2 was shown to produce atomic oxygen [3]. To investigate the significance of the molecular oxygen contribution to the photolyt-

ically produced oxygen atoms in the methane–air diffusion flame, the photolysis laser was tuned to 226.05 nm and 225.63 nm, corresponding to excitation wavelengths for the $O_2(0, 3) R(31)$ and $O_2(2, 4) P(21)$ lines, respectively [5]. No significant change of the spatial profile was observed, suggesting that any contribution to the photolytically produced O atom from O_2 is overwhelmed by a more significant production channel.

It is not surprising that we were not able to detect photolytic interference from O_2 in this flame. Due to the temperature and molecular oxygen profiles in the flame, significant Schumann–Runge absorption is expected only in the region of the flame where significant atomic oxygen is naturally present. The peak O-atom concentrations were $\sim 10^{16}$ cm^{-3}, and we expect O-atom concentrations resulting from photolysis of O_2 to be significantly less. In [3], a pump-probe experiment produced direct evidence of O-atom production from O_2 in the exhaust of a lean ($\phi = 0.25$) H_2/O_2 flame at atmospheric pressure. In that flame, however, the O_2 mole fraction was approximately 50% and measurements were performed 6 mm from the burner surface where the O-atom concentration is very small, so that the experiment was very sensitive to photolytic production of atomic oxygen. Even though a factor of 10 increase in the O-atom concentration was induced by the photolysis laser with a tightly focused 1.5-mJ pulse at 221.2 nm, we expect that the pho-

tolytic production was significantly less than 10^{15} cm^{-3}. In a single-laser experiment conducted in a low-pressure flame, Goldsmith [3] was unable to detect photolytically produced O atoms, presumably because there was only a few per cent of O_2 and the concentration of the photolytically produced O atoms was significantly less than that of the naturally occurring O atoms in the region probed ($> 5 \times 10^{14}$ cm^{-3}). Another single-laser experiment, also described in [3], used an atmospheric pressure H_2/O_2 flame ($\phi = 0.8$) to demonstrate flattening of the axial profiles of the measured O-atom LIF signal as the laser energy was increased. The profiles were normalized by their respective signal levels at a position 1 mm from the burner surface in Fig. 2 of [3]. At least in part, the flattening was attributed to photolytic production of O atoms [3], but probably was significantly influenced by stimulated emission with increasing excitation energy as observed in [16]. From this perspective and in view of the findings in this study, it can be speculated that photolytic O-atom production via Schumann–Runge absorption and subsequent predissociation is of less importance in hydrocarbon flames than O-atom production via photolysis of another precursor.

In hydrocarbon flames, CO_2 is a potential photolytic precursor. Vibrationally excited CO_2 was shown to photochemically produce CO via a single-photon transition at 230 nm in [20]. There is an equal yield of atomic oxygen from this process, and our observations are consistent with this mechanism. We observed no structure in the wavelength dependence of the oxygen-atom production at 226 nm, in accordance with absorption spectra measured in shock-heated CO_2 [21, 22]. Furthermore, we observed a linear dependence of the oxygen-atom production on the photolysis laser energy, indicating a single-photon process.

Figure 3 presents the results of a simple model used to support the assertion that CO_2 is the dominant photolytic precursor of atomic oxygen in this flame. Measured temperature and numerically simulated CO_2 profiles [14] were used in conjunction with the measured absorption cross section [22] to calculate the number density of excited-state CO_2 ($N_{CO_2^*}$) due to the photolysis laser. The
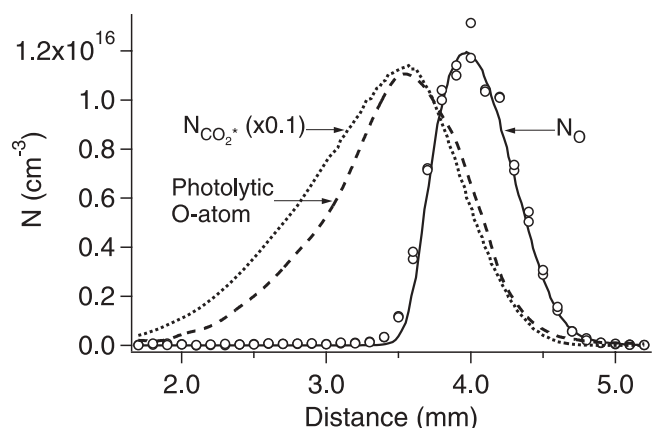
FIGURE 3 Modeled number-density profiles of excited-state CO_2 (*dotted*) and O (*solid*) and scaled LIF measurements corresponding to naturally occurring (*open circles*) and photolytically produced (*dashed curve*) atomic oxygen

calculated profile is shown as the dotted curve in Fig. 3. The numerically simulated atomic oxygen profile is shown as the solid curve, with the scaled LIF data shown as open circles. The measured photolysis signal is shown as the dashed curve. The spatial profile of the photolysis signal agrees very well with the computed $N_{CO_2^*}$ profile, and peak scaling suggests that approximately 10% of the CO_2^* molecules dissociate to produce $O\,2p\ ^3P$ under these conditions. The slight disagreement between the two profiles on the fuel side of the peak may be due to more efficient fluorescence quenching in the cooler fuel [7, 8].

4   Conclusions

The source photochemical interferences that can occur during two-photon LIF measurements of oxygen atoms in hydrocarbon-fueled flames were investigated. A weak ps probe laser was used to measure relative oxygen-atom concentrations in a well-documented laminar diffusion flame. The LIF measurements were unperturbed by stimulated emission, fluorescence interferences, and photochemical

effects. The measured profile coincided very well with a numerically simulated profile. Subsequently, an intense photolysis laser generated an oxygen-atom concentration of the same order of magnitude as the naturally occurring concentration. By scanning the wavelength of the photolysis laser it was shown that the absorption spectrum of the precursor molecule did not exhibit a discrete-line structure around 226 nm. In particular, photolysis of O_2 via Schumann–Runge transitions was shown to be negligible. Photolytic production of atomic oxygen depended linearly on the photolysis laser pulse energy, indicating a single-photon photolysis process. The laser-excited CO_2^* profile was calculated using the most recent data on the CO_2 absorption cross section, and demonstrated excellent agreement with the photolytically produced oxygen-atom profile. All of these results are consistent with vibrationally hot CO_2 being the photolytic precursor molecule responsible for atomic oxygen production at 226 nm in a CH_4/air diffusion flame.

REFERENCES

1 W.K. Bischel, B.E. Perry, D.R. Crosley: Chem. Phys. Lett. **82**, 85 (1981)
2 M. Aldén, H. Edner, P. Grafström, S. Svanberg: Opt. Commun. **42**, 244 (1982)
3 J.E.M. Goldsmith: Appl. Opt. **26**, 3566 (1987)
4 U. Meier, J. Bittner, K. Kohse-Höinghaus, T. Just: Proc. Combust. Inst. **22**, 1887 (1988)
5 I.J. Wysong, J.B. Jeffries, D.R. Crosley: Opt. Lett. **14**, 767 (1989)
6 K.C. Smyth, P.J.H. Tjossem: Appl. Phys. B **50**, 499 (1990)
7 K.C. Smyth, P.J.H. Tjossem: Proc. Combust. Inst. **23**, 1829 (1990)
8 L. Gasnot, P. Desgroux, J.F. Pauwels, L.R. Sochet: Appl. Phys. B **65**, 639 (1997)
9 U. Meier, K. Kohse-Höinghaus, T. Just: Chem. Phys. Lett. **126**, 567 (1986)
10 A.W. Miziolek, M.A. DeWilde: Opt. Lett. **9**, 390 (1984)
11 D.L. van Oostendorp, H.B. Levinsky, C.E. van der Meij, R.A.A.M. Jacobs, W.T.A. Borghols: Appl. Opt. **32**, 4636 (1993)
12 H. Tsuji: Prog. Energy Combust. Sci. **8**, 93 (1982)
13 V. Sick, F. Hildenbrand, P. Lindstedt: Proc. Combust. Inst. **27**, 1401 (1998)
14 J.J. Driscoll, V. Sick, P.E. Schrader, R.L. Farrow: Proc. Combust. Inst. **29**, 2719 (2002)
15 T.B. Settersten, A. Dreizler, R.L. Farrow: J. Chem. Phys. **117**, 3173 (2002)
16 M. Aldén, U. Westblom, J.E.M. Goldsmith: Opt. Lett. **14**, 305 (1989)
17 J. Bittner, K. Kohse-Höinghaus, U. Meier, T. Just: Chem. Phys. Lett. **143**, 571 (1988)
18 P.J. Dagdigian, B.E. Forch, A.W. Miziolek: Chem. Phys. Lett. **148**, 299 (1988)
19 F. Ossler, J. Larsson, M. Aldén: Chem. Phys. Lett. **250**, 287 (1996)
20 A.P. Nefedov, V.A. Sinel´shchikov, A.D. Usachev, A.V. Zobnin: Appl. Opt. **37**, 7729 (1998)
21 C. Schulz, J.D. Koch, D.F. Davidson, J.B. Jeffries, R.K. Hanson: Chem. Phys. Lett. **355**, 82 (2002)
22 C. Schulz, J.B. Jeffries, D.F. Davidson, J.D. Koch, J. Wolfrum, R.K. Hanson: Proc. Combust. Inst. **29**, 2735 (2002)